Autodetachment and vibronic coupled photodetachment transitions of $C_2H_3O^-$

Stephen Gibson and Benjamin Laws

Australian National University
Canberra

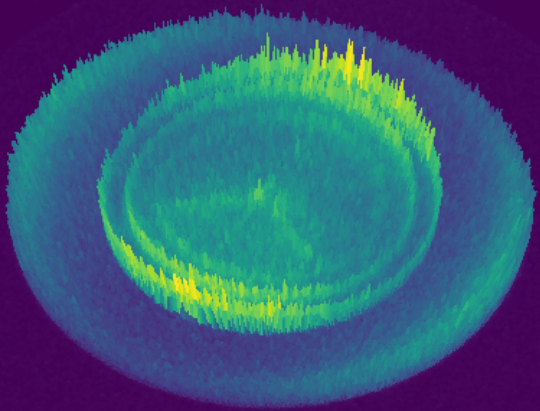

ISMS June 19, 2019

- Historical
- $C_2H_3O^-$ PES decomposition
- $C_2H_3O^-$ PAD decomposition
- vibronic coupling
- dipole-bound states

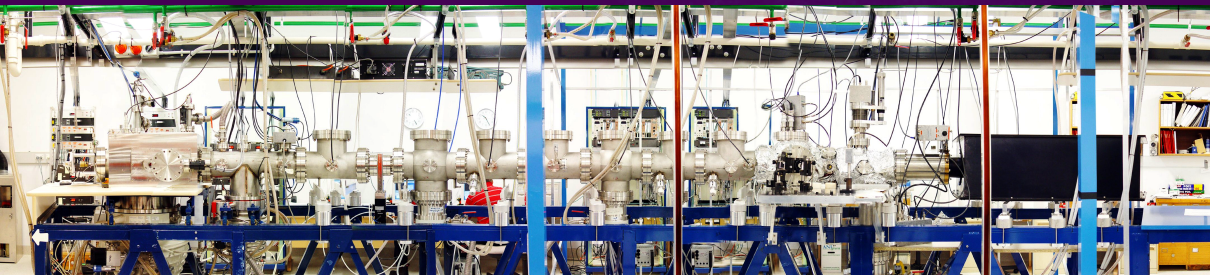

Historical
(some) $C_2H_3O^-/C_2H_3O$ spectroscopy

- First evidence for dipole-bound excited states (DBS)
- Herzberg-Teller bands in $\tilde{A} - \tilde{X}$

Total photoelectron yield

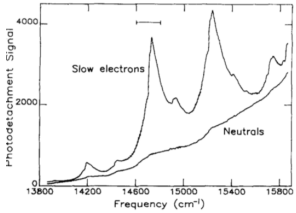

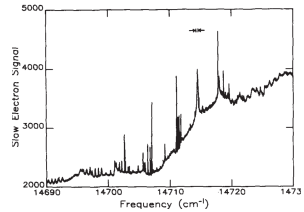

Ervin and Lineberger J Phys Chem **95** 1167 (1991)

Lineberger

Neumark

SEVI

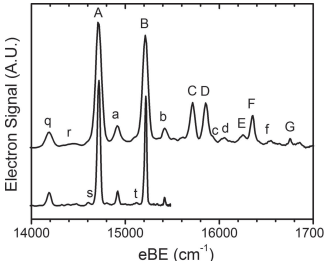

Yacovitch, Garand, Neumark J Chem Phys **130** 244309 (2009)

Miller

CRDS

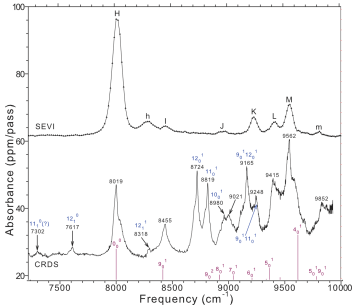

Thomas, Chhantyal-Pun, Kline, and Miller
J Chem Phys **132** 114302 (2010)

HR-PEI measurements - vinoxide photoelectron spectrum (PES)

$C_2H_3O(\tilde{A}^2A', \tilde{X}^2A'') \leftarrow C_2H_3O^-(\tilde{X}^1A') + h\nu$

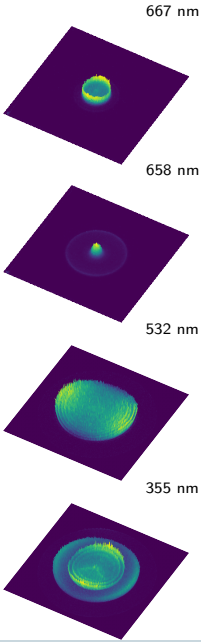

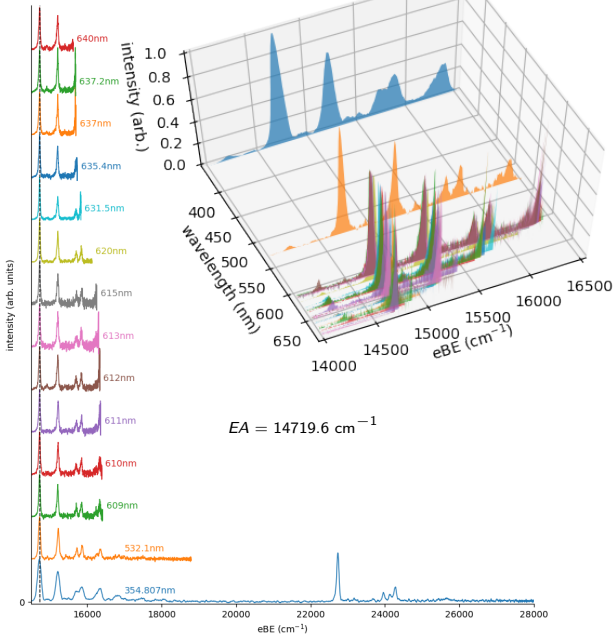

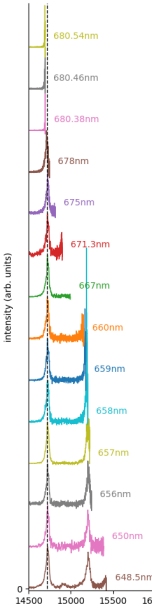

PES
comparison

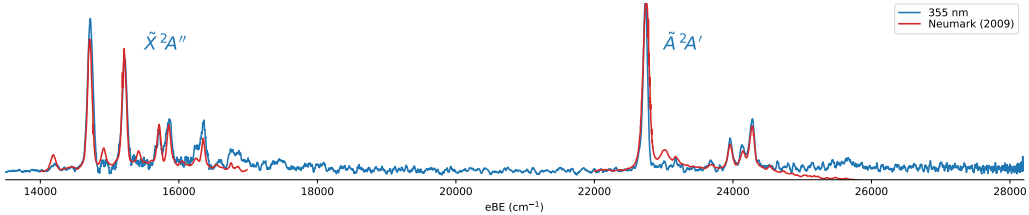

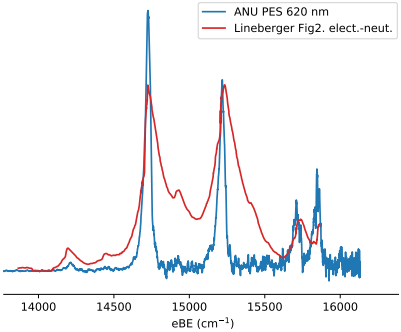

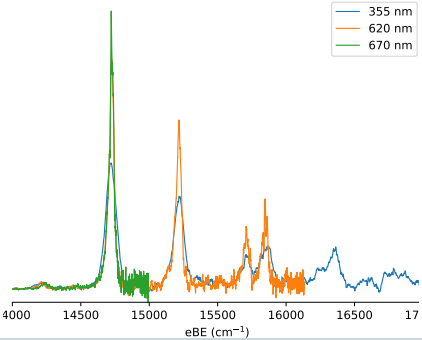

PES

Structure - $\tilde{X}\,^2A''$ rotational

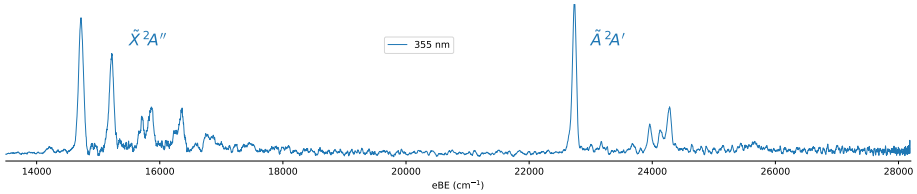

rotational structure

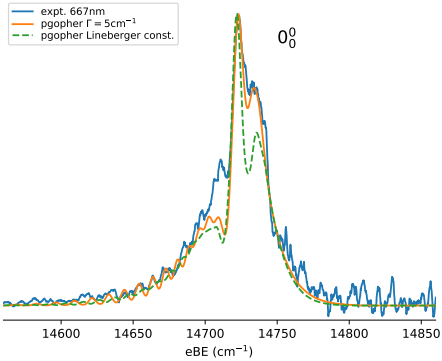

C_s

cm^{-1}	A	B	C
$\tilde{X}\,^2A''$	2.1952(2.219)	0.3737(0.3758)	0.3193(0.3207)
$\tilde{X}\,^1A'$	2.5162(2.493)	0.3545(0.3622)	0.3107(0.3159)

PES

Structure - $\tilde{X}\,^2A''$ rotational

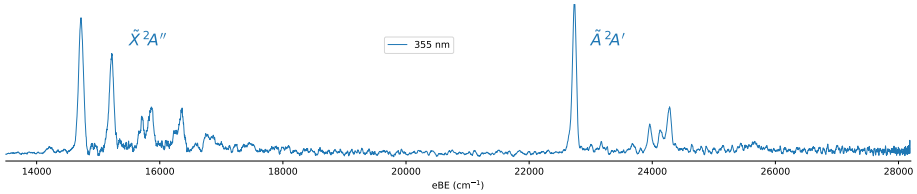

rotational structure

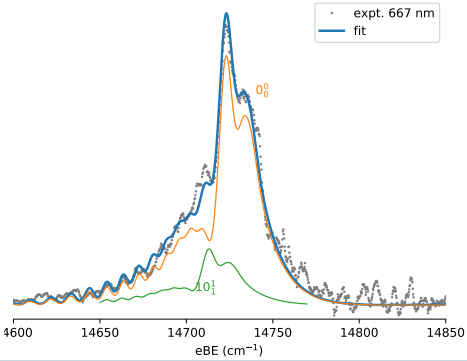

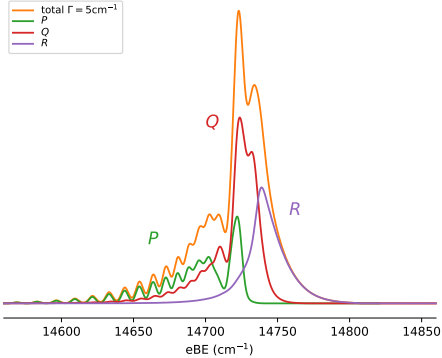

PES $\tilde{X}\,^2A''$

normal-mode decomposition

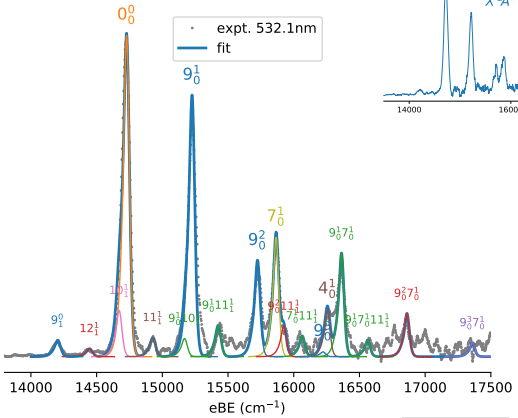

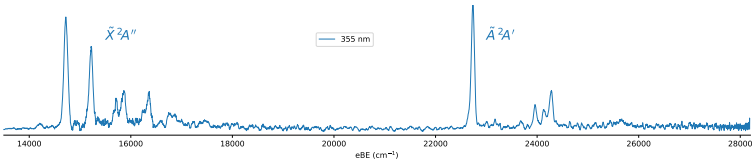

vibrational modes - *ab initio*, expt.-Neumark, expt.-ANU

mode	type	sym.	$\tilde{X}\,^1A'$	$\tilde{X}\,^2A''$	
ω_1	CH_2 asym. stretch	a'	3068	3148	
ω_2	CH_2 sym. stretch	a'	2986	3037	
ω_3	CH(3) stretch	a'	2585	2849	
ω_4	CO stretch	a'	1550	1528	
ω_5	CH_2 bend	a'	1396	1486	
ω_6	HCO bend	a'	1550	1366	
ω_7	CC stretch	a'	1182	1137	1135(1)
ω_8	CH_2 rock	a'	960	957	
ω_9	CCO bend	a'	524	498	502(1)
ω_{10}	CH(3) out plane wag	a''	943	886	
ω_{11}	all CH wag	a''	358	557	
ω_{12}	CH_2 twist	a''	686	404	

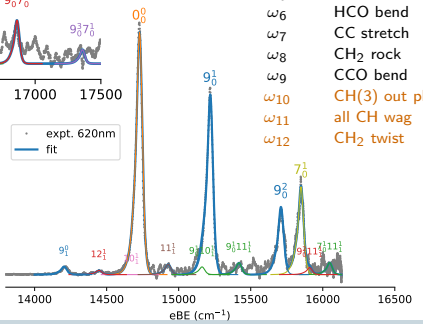

PES C_2H_3O $\tilde{A}\,^2A' \leftarrow C_2H_3O^-$ $\tilde{X}\,^1A'$

excited state: vibrational normal-mode decomposition

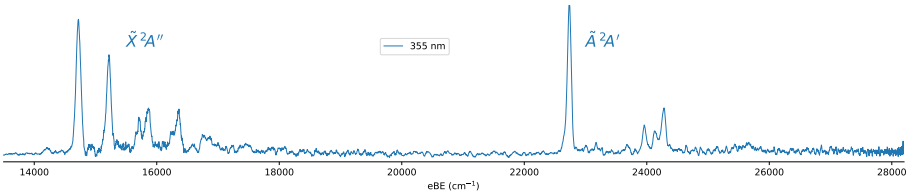

vibrational modes - *ab initio*, expt.-Miller, expt.-ANU

mode	type	sym.	$\tilde{A}\,^2A'$	
ω_1	CH_2 asym. stretch	a'	3068	
ω_2	CH_2 sym. stretch	a'	2986	
ω_3	CH(3) stretch	a'	2585	
ω_4	CC stretch	a'	1533	1541(1)
ω_5	CH_2 scissors	a'	1403	1397(1)
ω_6	HCO bend	a'	1218	1221(1)
ω_7	CO stretch	a'	1002	
ω_8	CH_2 rock	a'	961	
ω_9	CCO bend	a'	436	
ω_{10}	out-of-plane bend	a''	946	
ω_{11}	out-of-plane mode	a''	799	
ω_{12}	out-of-plane mode	a''	705	

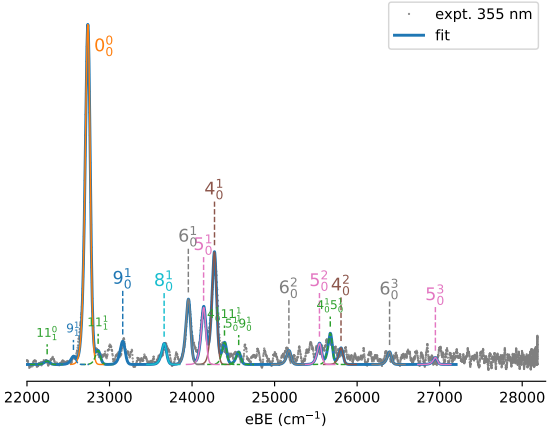

PES C_2H_3O $\tilde{A}\,^2A' \leftarrow C_2H_3O^-$ $\tilde{X}\,^1A', \tilde{X}\,^2A''$

PES vs CRDS

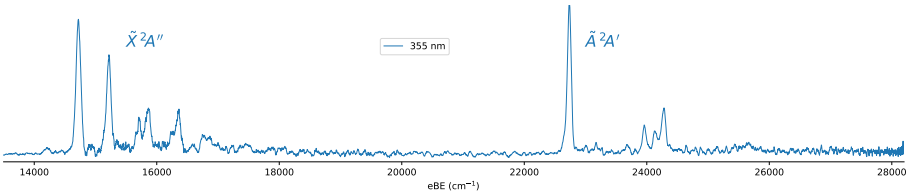

vibrational modes - *ab initio*, expt.-Miller, expt.-ANU

mode	type	sym.	$\tilde{A}\,^2A'$	
ω_1	CH_2 asym. stretch	a'	3068	
ω_2	CH_2 sym. stretch	a'	2986	
ω_3	CH(3) stretch	a'	2585	
ω_4	CC stretch	a'	1533	1541(1)
ω_5	CH_2 scissors	a'	1403	1397(1)
ω_6	HCO bend	a'	1218	1221(1)
ω_7	CO stretch	a'	1002	
ω_8	CH_2 rock	a'	961	
ω_9	CCO bend	a'	436	
ω_{10}	out-of-plane bend	a''	946	
ω_{11}	out-of-plane mode	a''	799	
ω_{12}	out-of-plane mode	a''	705	

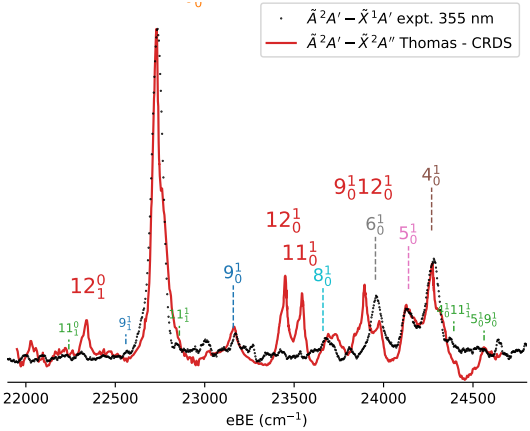

Photoelectron angular distribution (PAD)

Signatures

355 nm

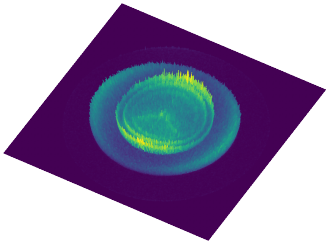

532 nm

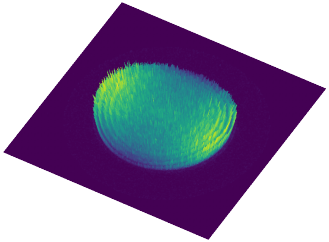

$$I(\epsilon, \theta) = \frac{\sigma(\epsilon)}{4\pi}[1 + \beta(\epsilon)P_2(\cos\theta)]$$

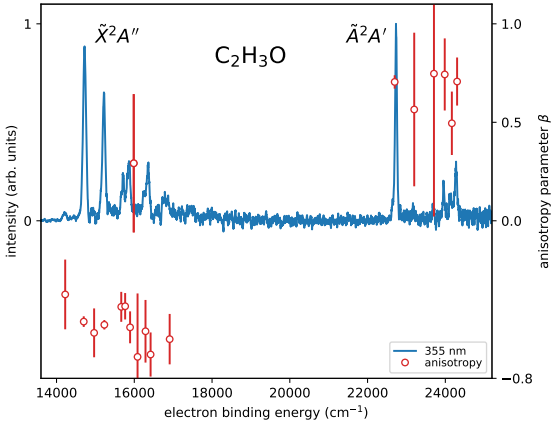

Photoelectron angular distribution (PAD)

Slices

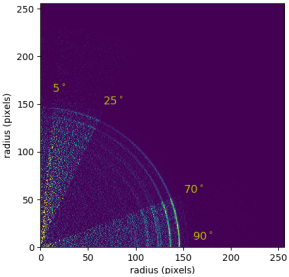

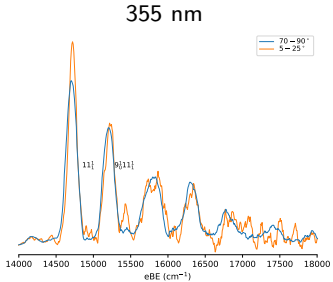

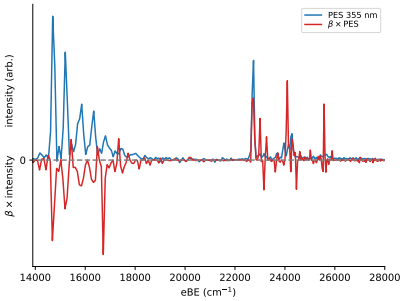

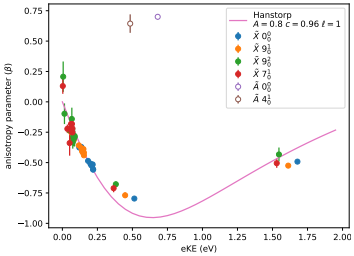

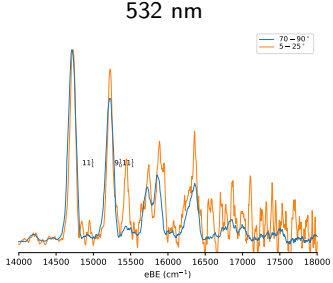

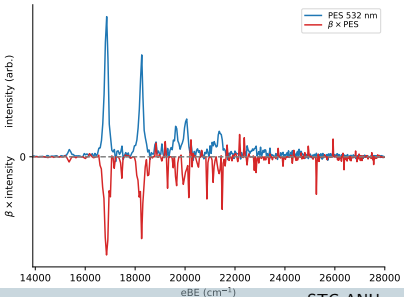

Dipole-bound state enhancement

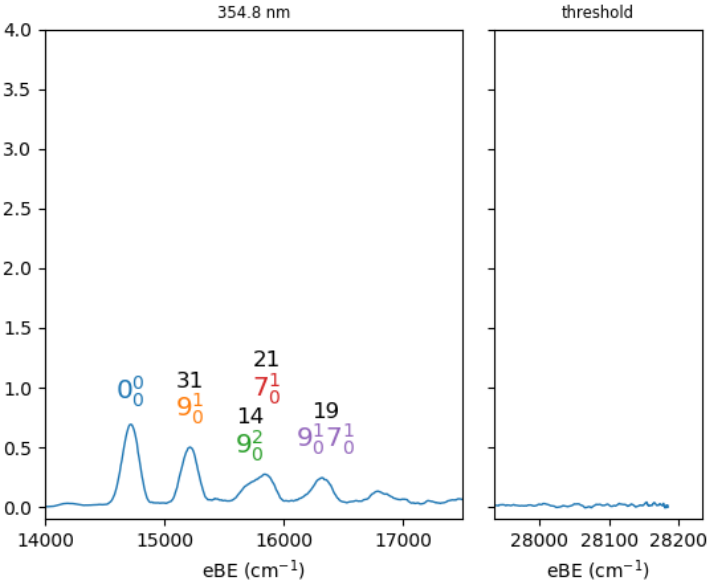

$\simeq$ area relative to 0_0^0

Dipole-bound state enhancement

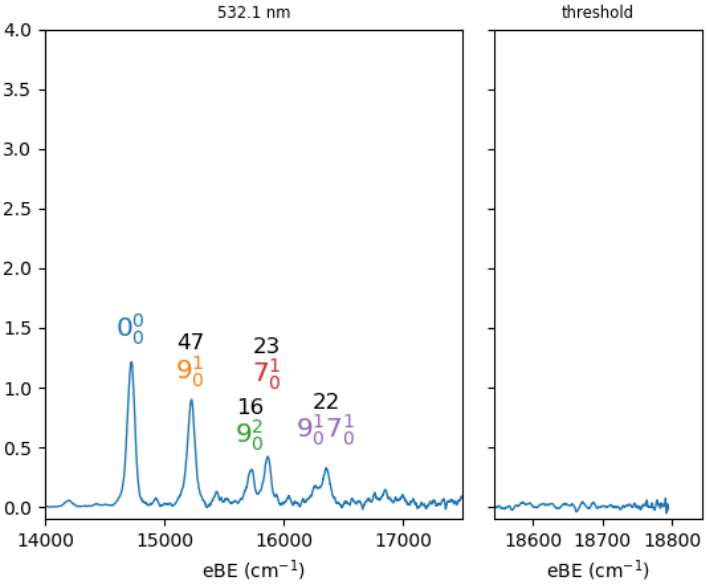

$\simeq$ area relative to 0_0^0

Dipole-bound state enhancement

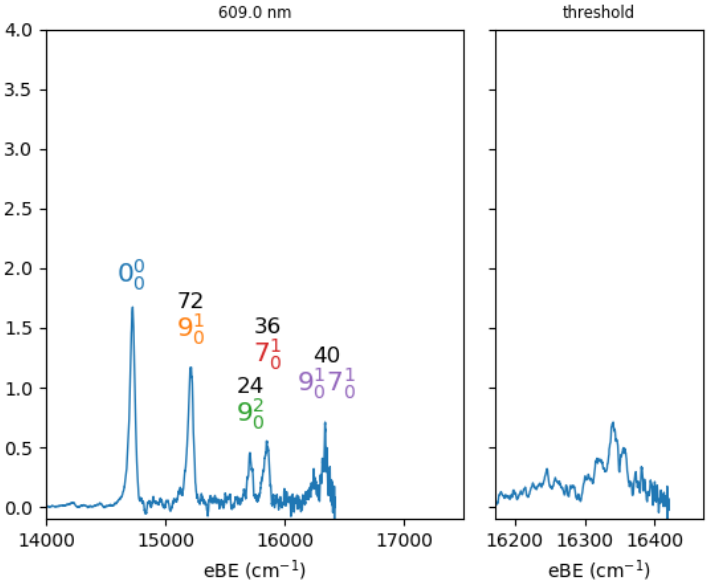

$\simeq$ area relative to 0_0^0

Dipole-bound state enhancement

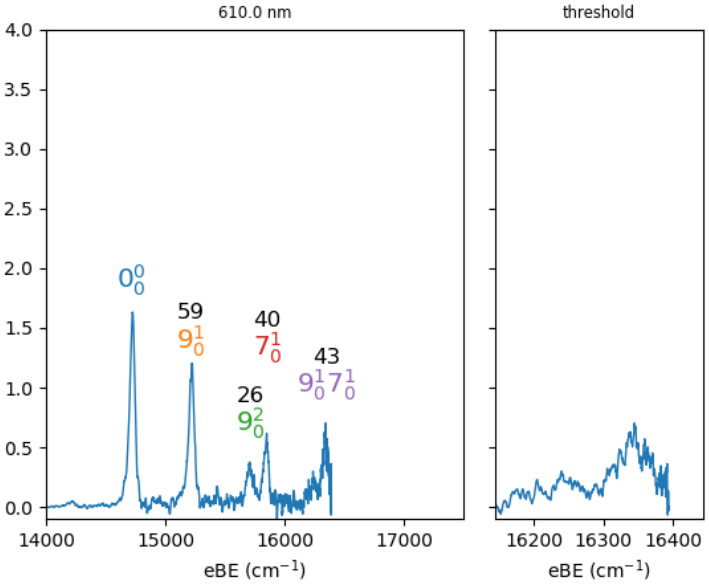

$\simeq$ area relative to 0_0^0

Dipole-bound state enhancement

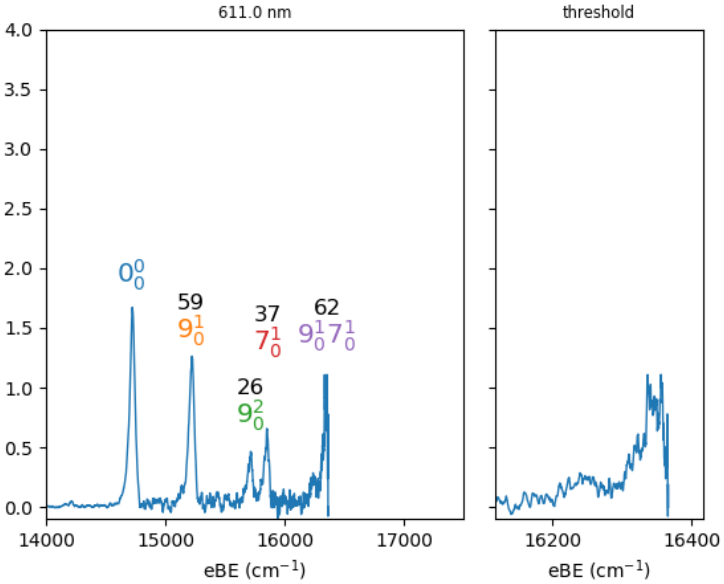

$\simeq$ area relative to 0_0^0

Dipole-bound state enhancement

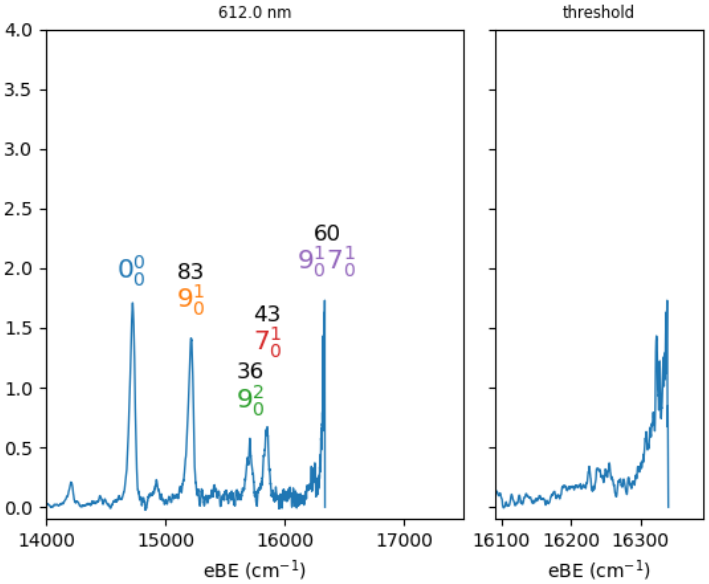

$\simeq$ area relative to 0_0^0

Dipole-bound state enhancement

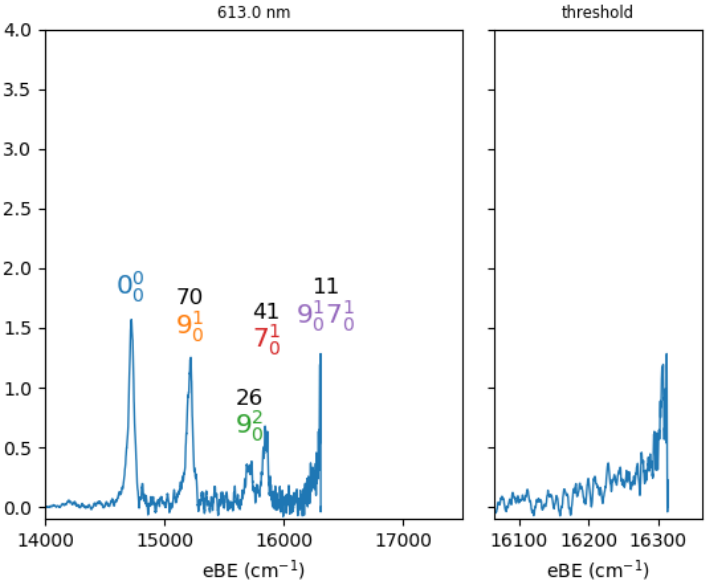

$\simeq$ area relative to 0_0^0

Dipole-bound state enhancement

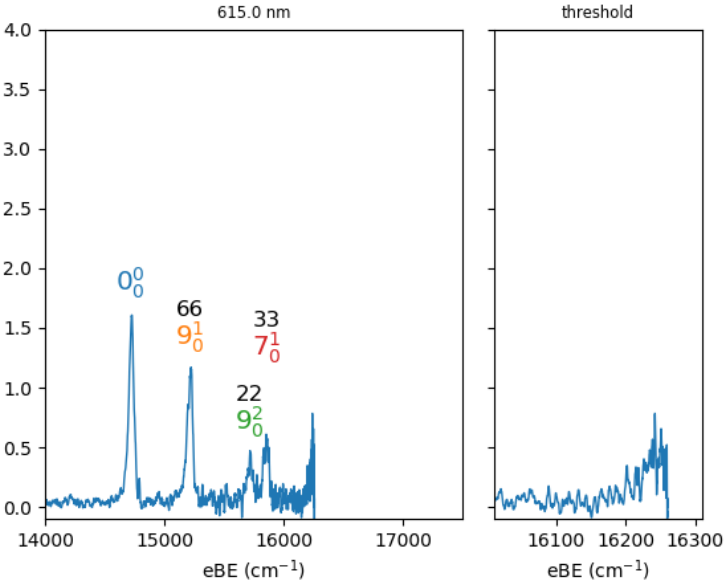

$\simeq$ area relative to 0_0^0

Dipole-bound state enhancement

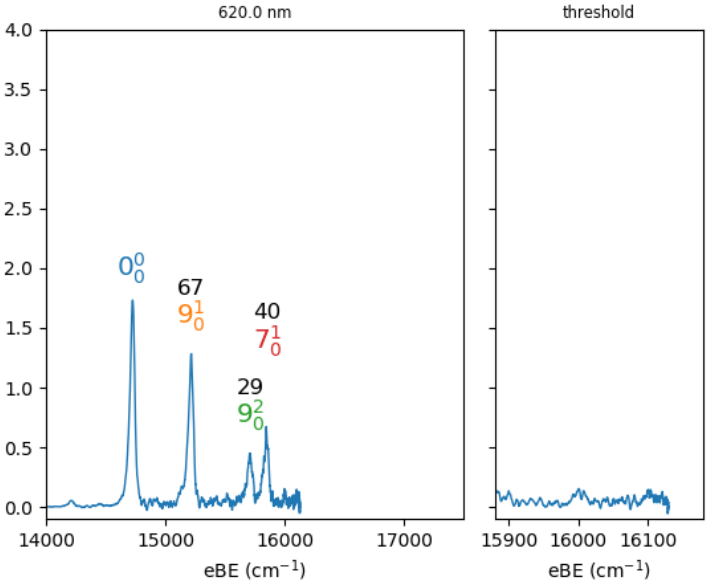

$\simeq$ area relative to 0_0^0

Dipole-bound state enhancement

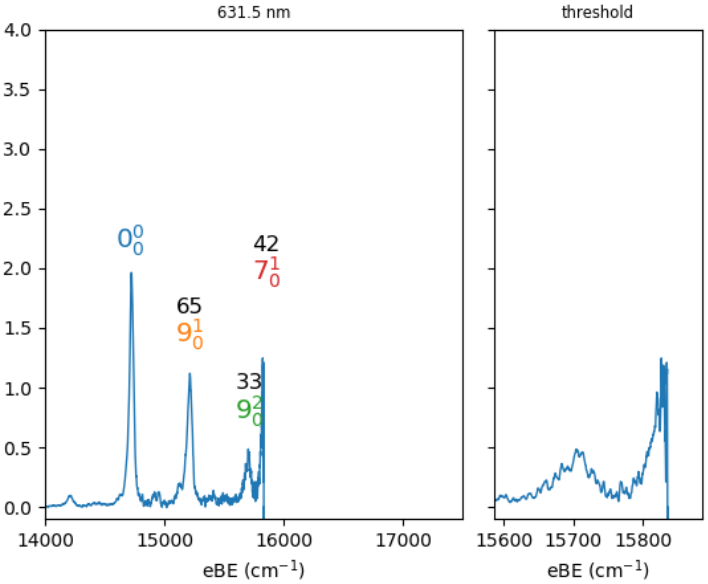

$\simeq$ area relative to 0_0^0

Dipole-bound state enhancement

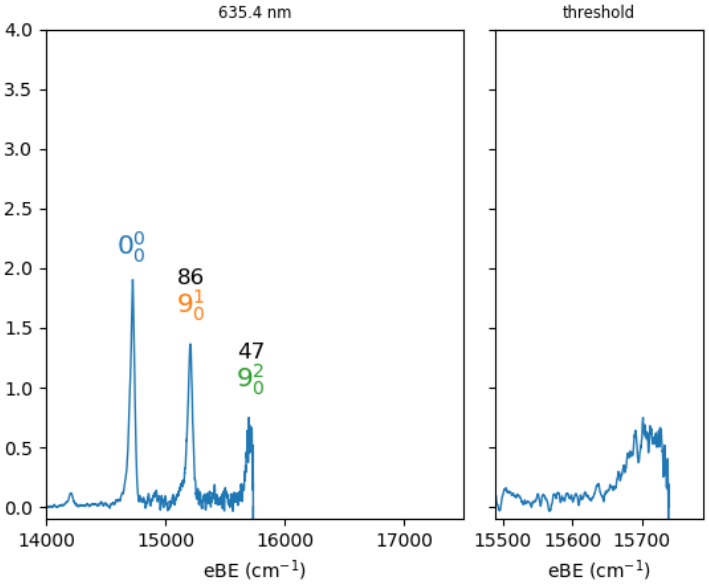

$\simeq$ area relative to 0_0^0

Dipole-bound state enhancement

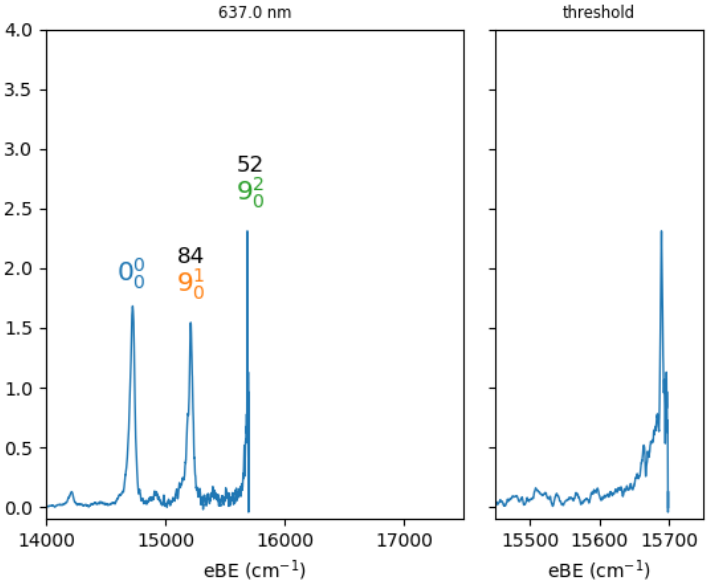

$\simeq$ area relative to 0_0^0

Dipole-bound state enhancement

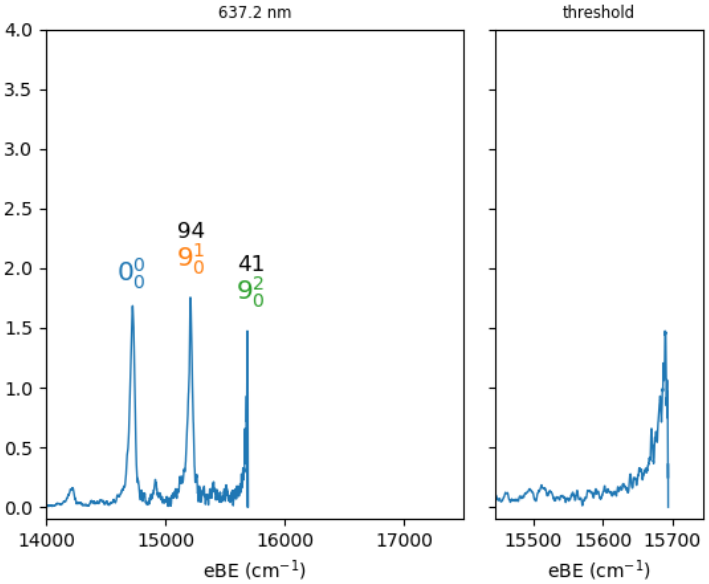

$\simeq$ area relative to 0_0^0

Dipole-bound state enhancement

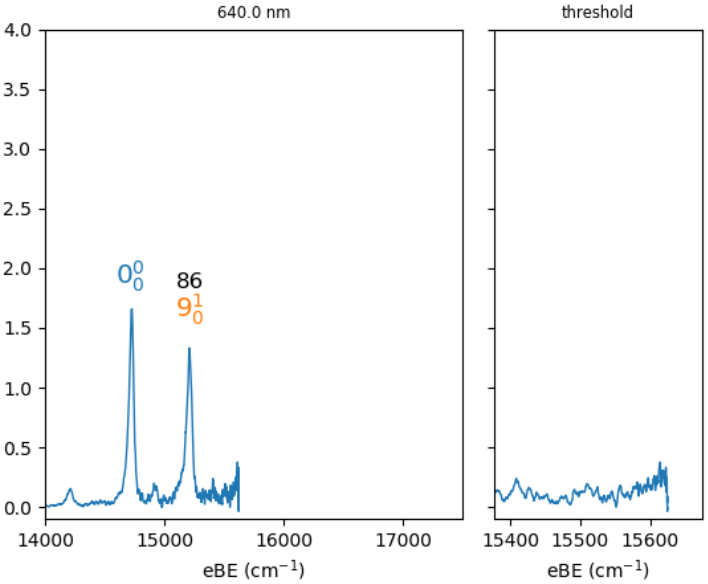

$\simeq$ area relative to 0_0^0

Dipole-bound state enhancement

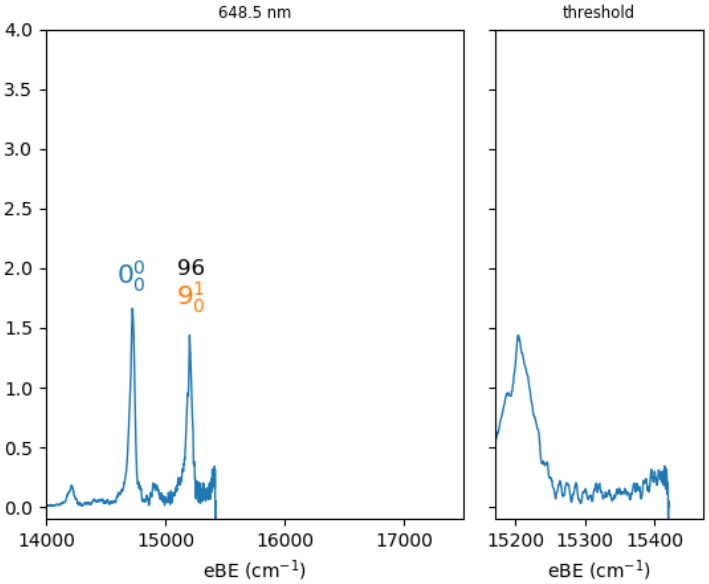

$\simeq$ area relative to 0_0^0

Dipole-bound state enhancement

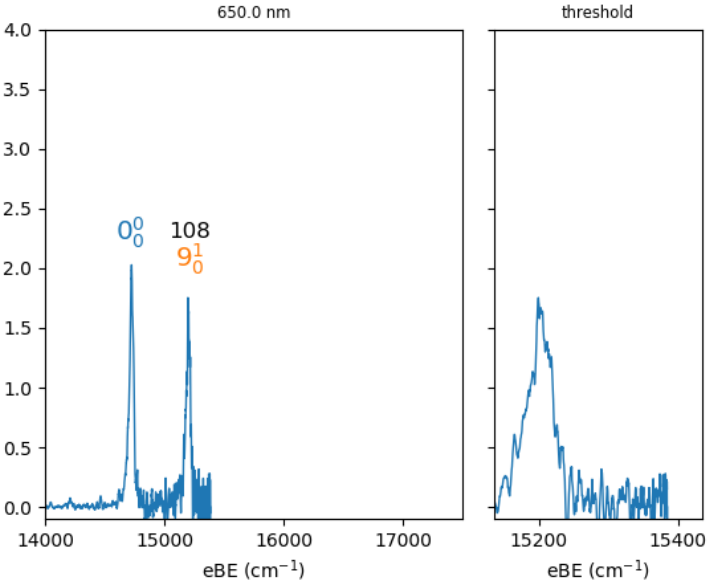

$\simeq$ area relative to 0_0^0

Dipole-bound state enhancement

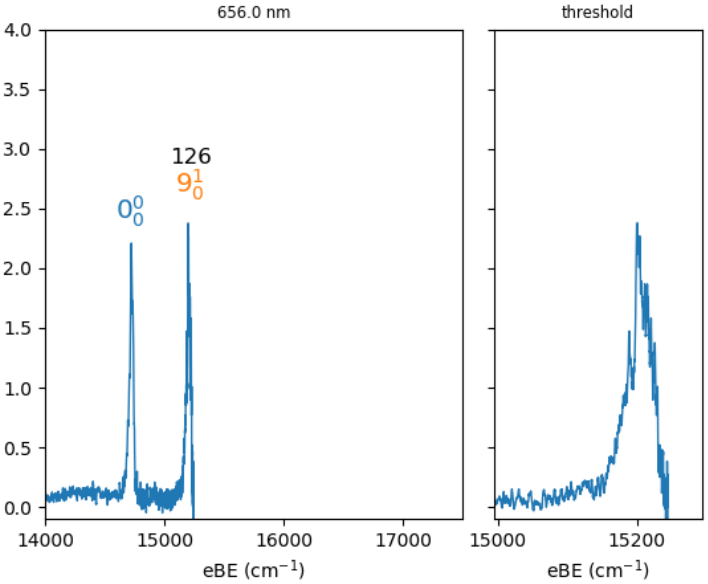

$\simeq$ area relative to 0^0_0

Dipole-bound state enhancement

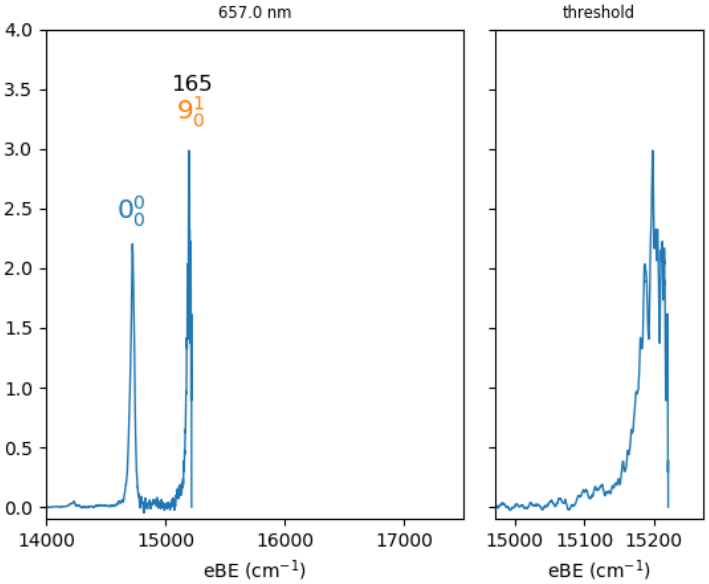

$\simeq$ area relative to 0^0_0

Dipole-bound state enhancement

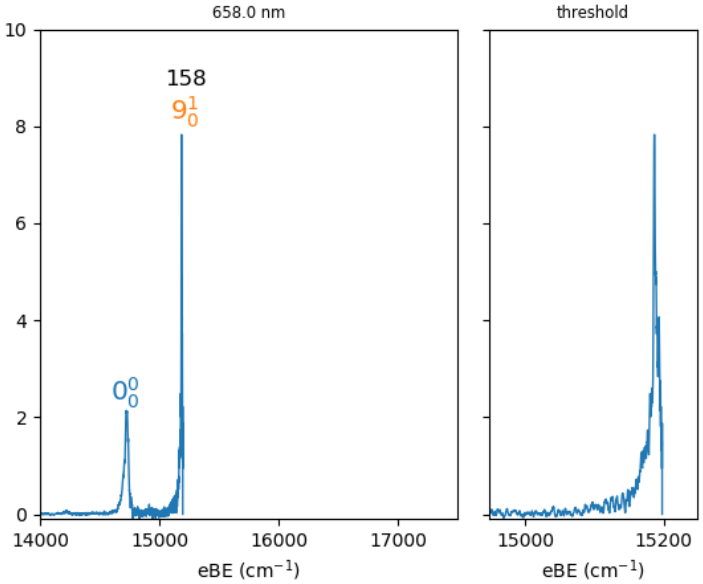

$\simeq$ area relative to 0^0_0

Dipole-bound state enhancement

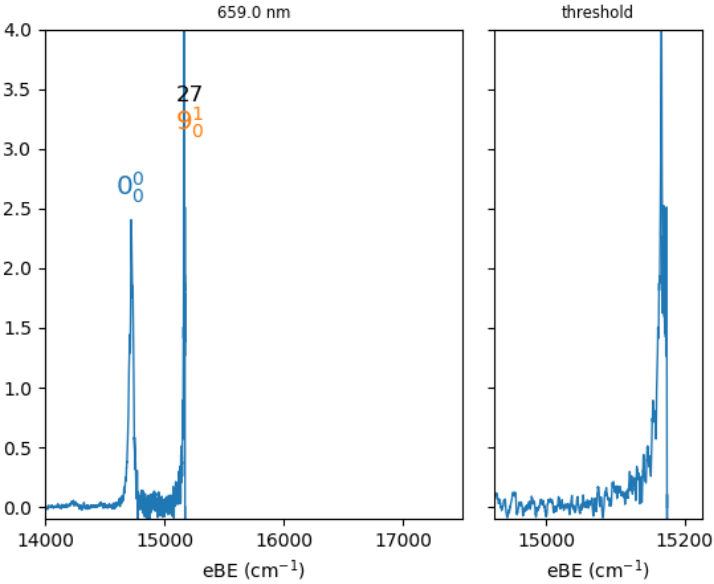

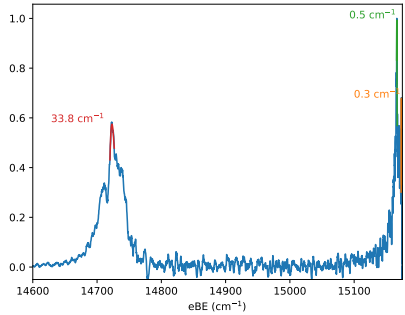

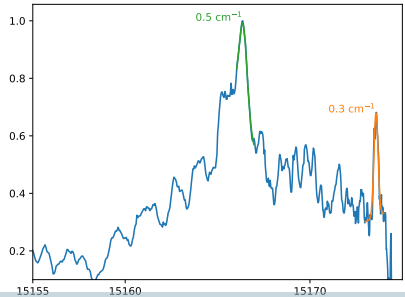

Dipole-bound state enhancement

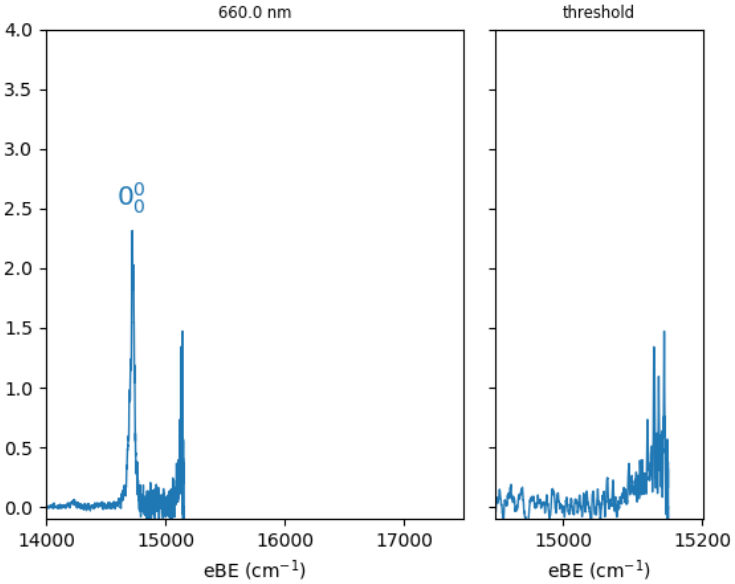

Dipole-bound state enhancement

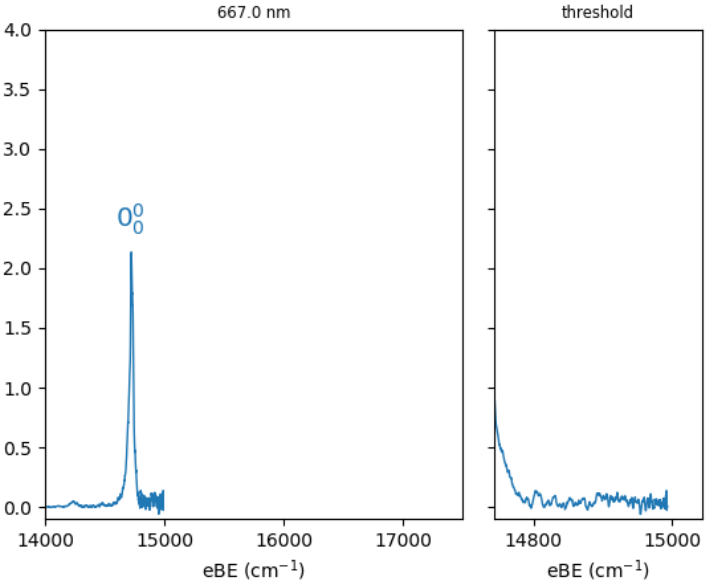

Dipole-bound state enhancement

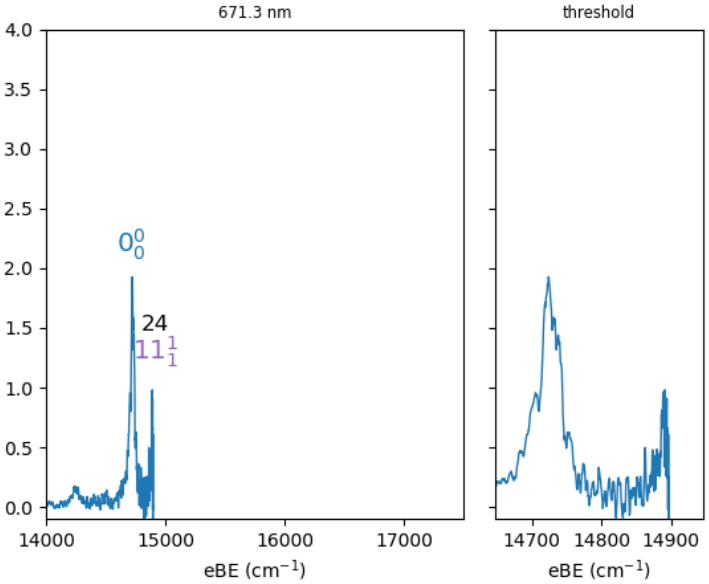

$\simeq$ area relative to 0_0^0

Dipole-bound state enhancement

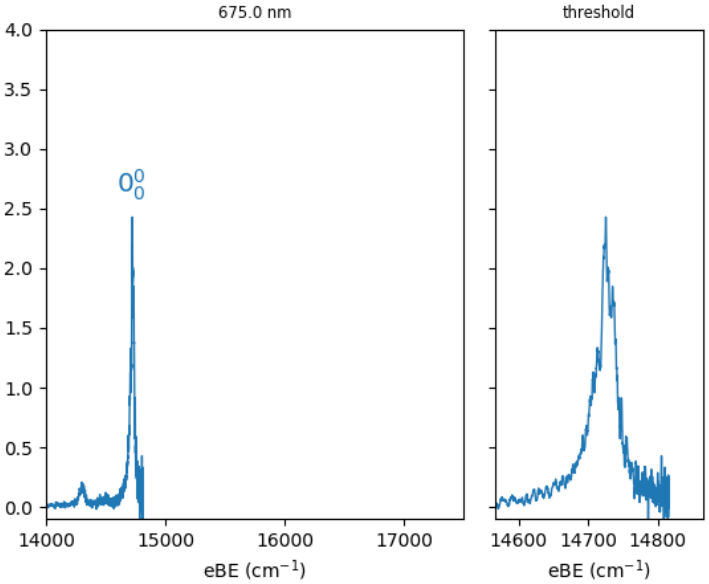

DBS: PES enhancement near threshold

9_0^1

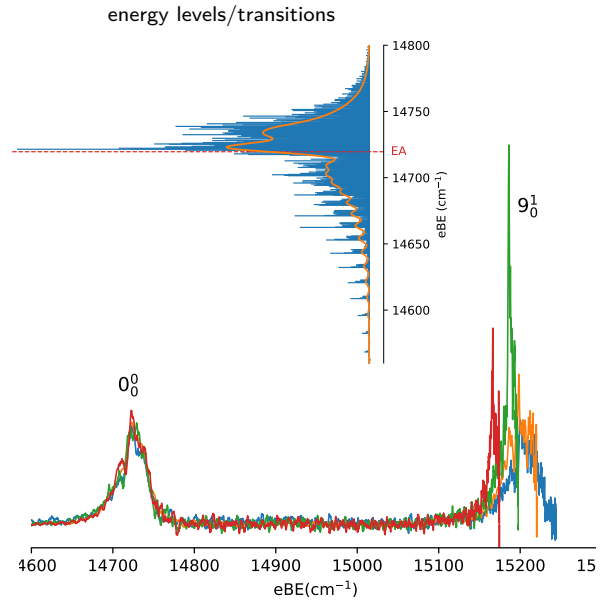

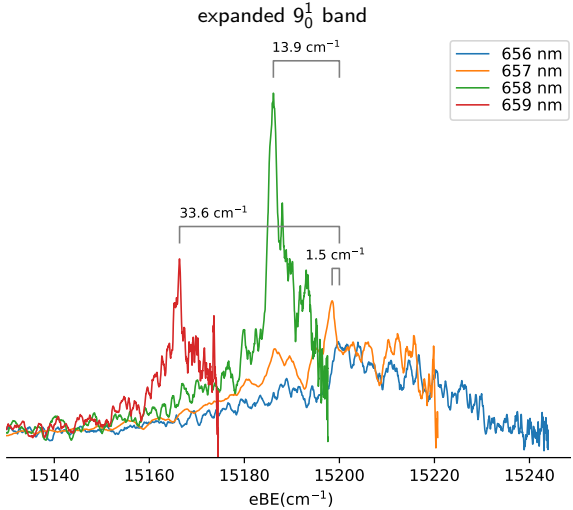

DBS near threshold

Origin 0_0^0

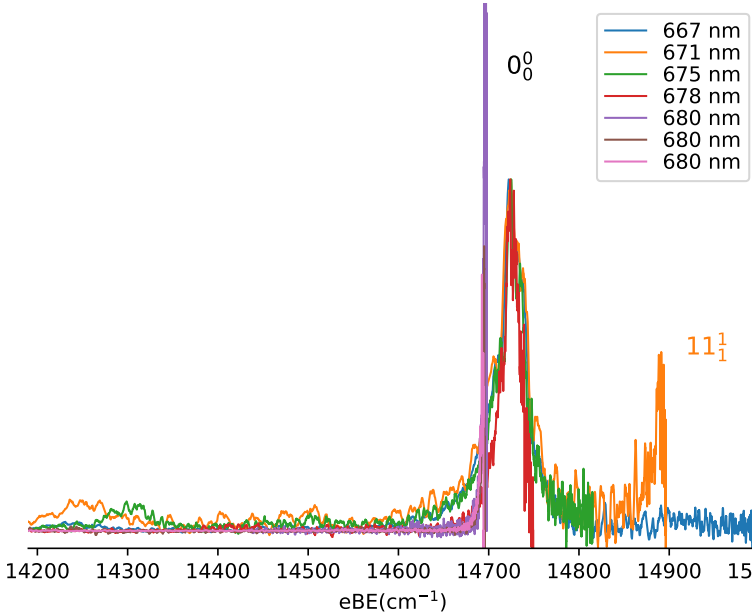

DBS vibrational coupling

9_0^1 enhancement

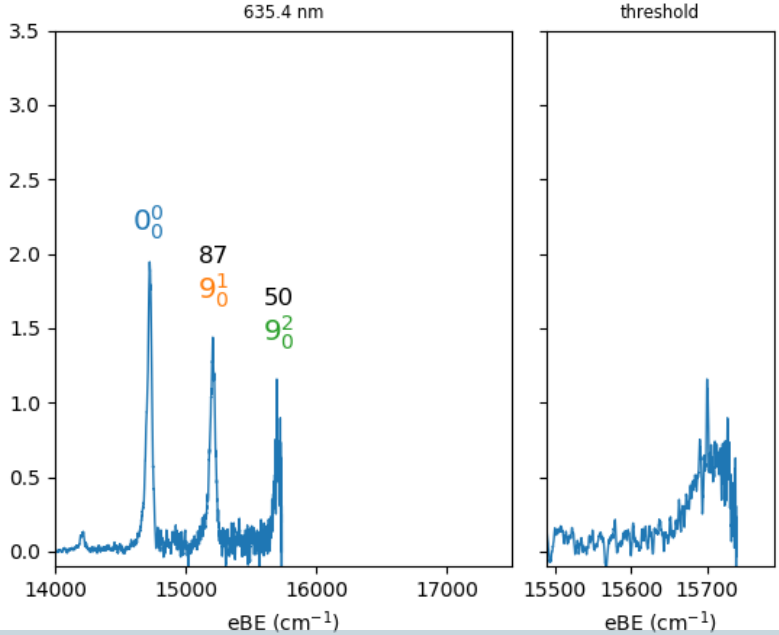

DBS vibrational coupling

9_0^1 enhancement

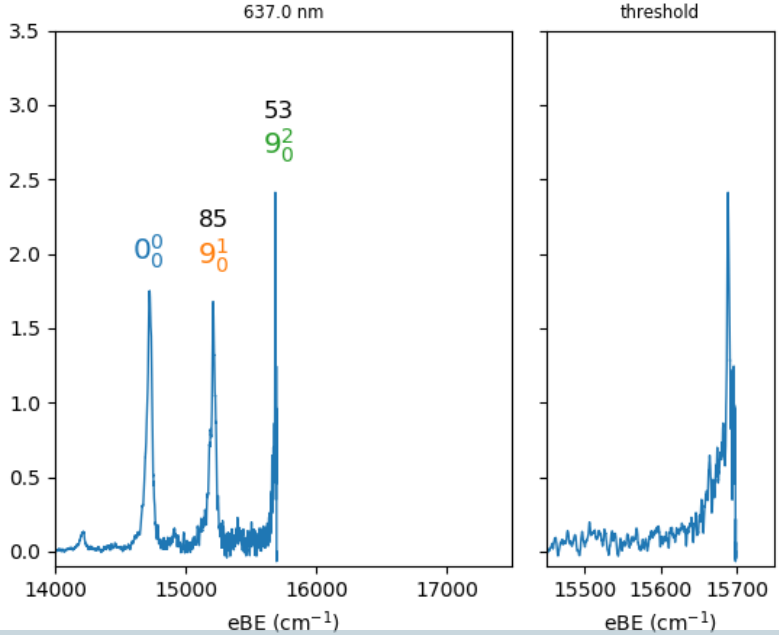

DBS vibrational coupling

9_0^1 enhancement

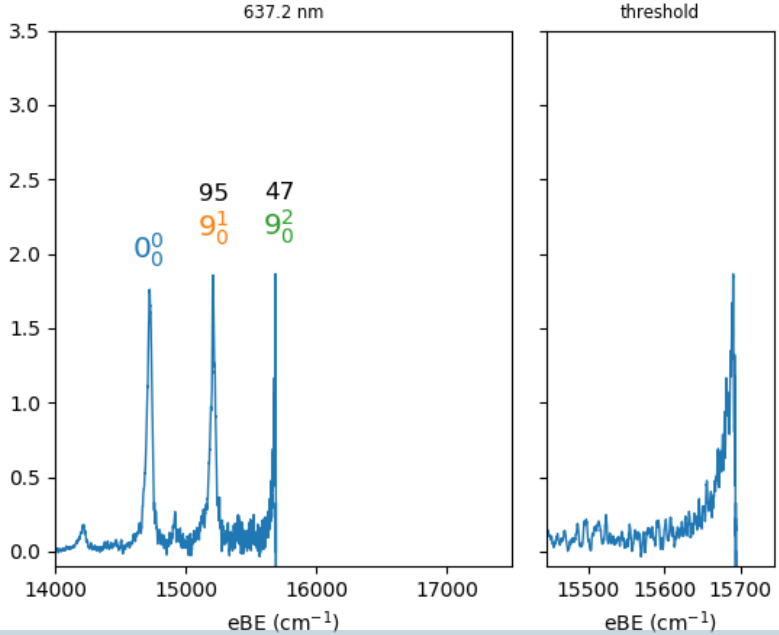

DBS vibrational coupling

9_0^1 enhancement

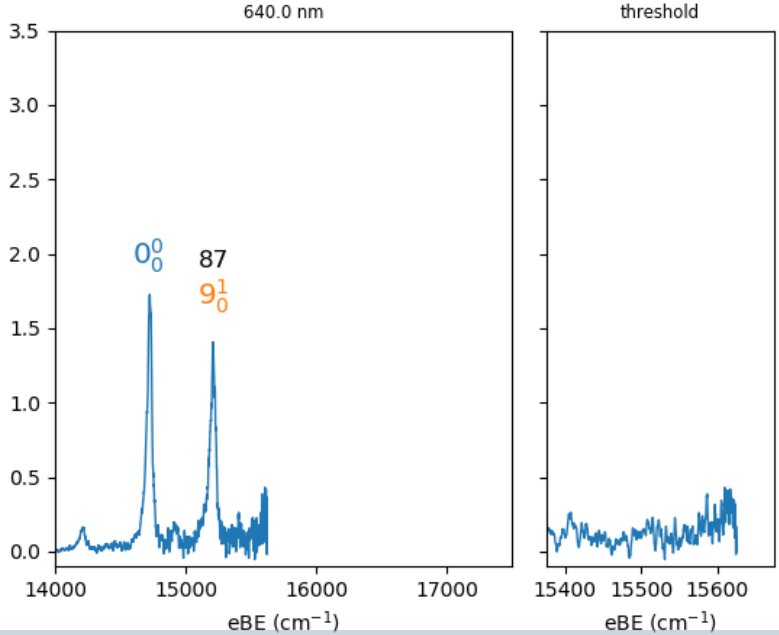

Summary and Conclusions

C_2H_3O ($\tilde{A}\,^2A', \tilde{X}\,^2A''$) $\leftarrow$ $C_2H_3O^-$ ($\tilde{X}\,^1A'$)

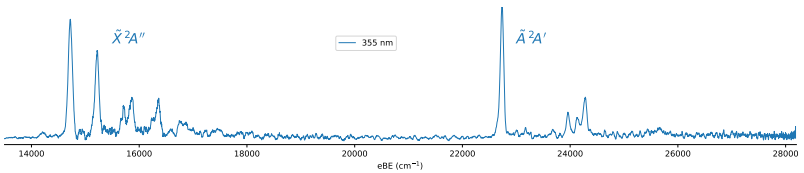

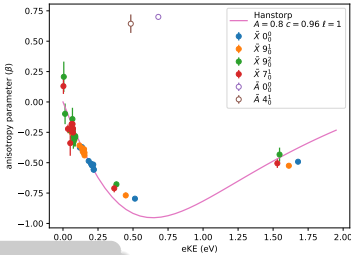

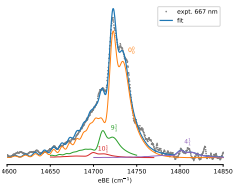

Summary/Conclusions

- HR-PEI measurements of $C_2H_3O^-$ photodetachment
- Origin band FWHM ~ 5 cm^{-1} - rotational envelope
- Anisotropy parameters determined
- (vibronic coupling - to be verified)
- DBS resonances
  - near theshold FWHM $\lesssim 0.5(1)$ cm^{-1}
  - resonance has a band shape - may be additional structure
- DBS mode enhancement

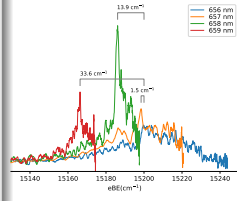

Acknowledgements

People

- Brenton Lewis (ANU)
- Steven Cavanagh (ANU)
- Robert Field (MIT)
- Richard Mabbs (Wash. U.)
- Andrei Sanov (Ariz. U.)

Technical

- Colin Dedman (electronic)
- Ross Trantor (mechanical)

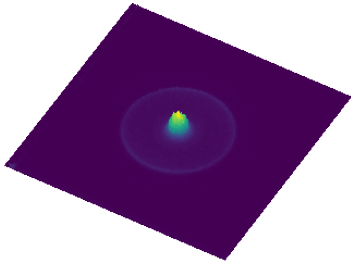

Open source software

- PyAbel - Abel transforms - github.com/PyAbel Rev. Sci. Instrum. paper in June
- NWChem - computational chemistry - github.com/nwchemgit/nwchem
- Pgopher - simulate rovibrational spectra - pgopher.chm.bris.ac.uk
- ezySpectrum - github.com/iopenshell/ezSpectrum
- Python and matplotlib - www.python.org and matplotlib.org
- PyDiatomic - Coupled-channel Schrödinger equation - github.com/stggh/PyDiatomic

Funding

- Australian Research Council DP160102585

End (Appendix)

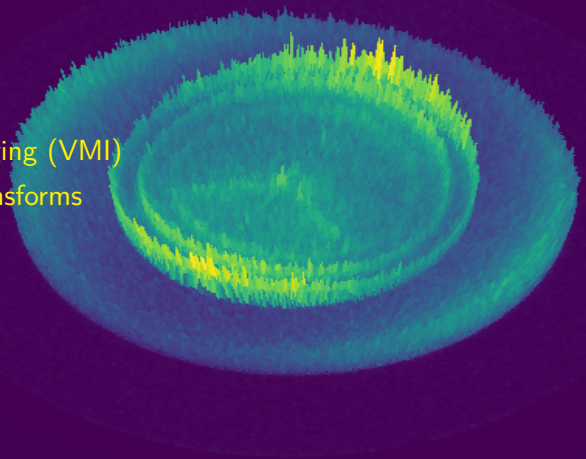

- Spectrometer
- Velocity-map imaging (VMI)
- PyAbel - Abel transforms

Spectrometer - photodetachment/photofragmentation

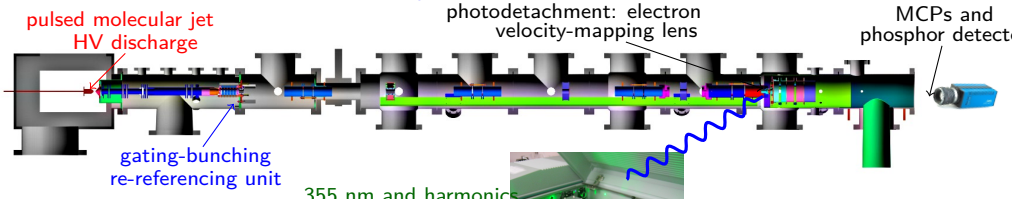

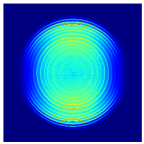

355 nm and harmonics
Nd:YAG laser

OPO laser 220 nm−1750 nm

Fast beam spectrometer:
Cyr PhD Thesis (UC Berkeley 1993)

Velocity-map imaging lens:
Eppink and Parker Rev Sci Instrum **68** 3477 (1997)

Gating-bunching-rereferencing unit:
(ANU) Dedman *et al.* Rev Sci Instrum **73** 2915 (2001)

Photodetachment:

$A^- + h\nu \rightarrow A^* + e^-$

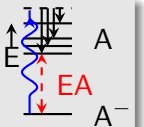

Velocity-map imaging
HR-PEI

VMI lens coaxial with ion-beam

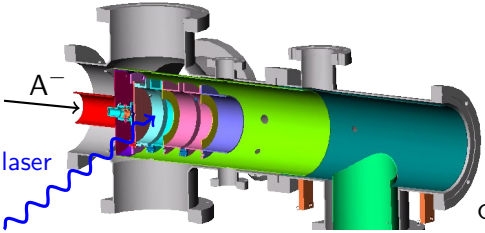

MCPs+phosphor

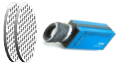

CCD camera 2048x2048 pixel

monochrome camera image

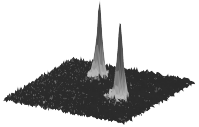

(x_i, y_i)

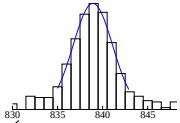

sub-pixel centroid

bin to image

circularize Gascooke (Flind U)

e^- trajectories

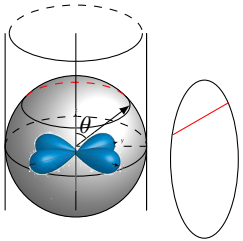

2D projection O_2^-

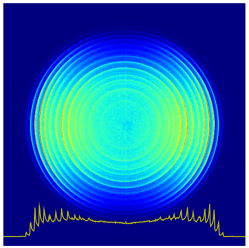

3D slice

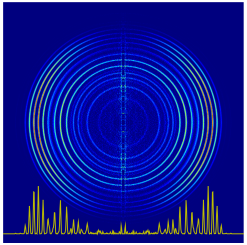

$\frac{\Delta E}{E} \sim$ constant $\rightarrow e^-$ speed

Inverse Abel transformation: **PyAbel**: https://github.com/PyAbel

PyAbel: Abel transform software

https://github.com/PyAbel

PyAbel README

build passing BUILD PASSING

Note: This readme is best viewed as part of the PyAbel Documentation.

Introduction

`PyAbel` is a Python package that provides functions for the forward and inverse Abel transforms. The forward Abel transform takes a slice of a cylindrically symmetric 3D object and provides the 2D projection of that object. The inverse abel transform takes a 2D projection and reconstructs a slice of the cylindrically symmetric 3D distribution.

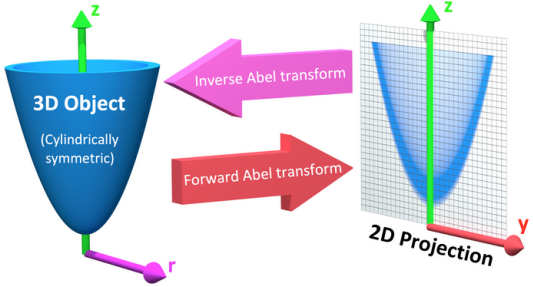

Inverse Abel transforms play an important role in analyzing the projections of angle-resolved photoelectron/photoion spectra, plasma plumes, flames, and solar occultation.

PyAbel provides efficient implementations of several Abel transform algorithms, as well as related tools for centering images, symmetrizing images, and calculating properties such as the radial intensity distribution and the anisotropy parameters.

Transform Methods

The outcome of the numerical Abel Transform depends on the exact method used. So far, PyAbel includes the following transform methods:

1. `basex` - Gaussian basis set expansion of Dribinski and co-workers.
2. `hansenlaw` - recursive method of Hansen and Law.
3. `direct` - numerical integration of the analytical Abel transform equations.
4. `two_point` - the "two point" method of Dasch and co-workers.
5. `three_point` - the "three point" method of Dasch and co-workers.
6. `onion_peeling` - the "onion peeling" deconvolution method of Dasch and co-workers.
7. `onion_bordas` - "onion peeling" or "back projection" method of Bordas *et al.* based on the MatLab code by Rallis and Wells *et al.*
8. `linbasex` - the 1D-spherical basis set expansion of Gerber *et al.*